Electronic Supplementary Material (ESI) for Journal of Materials Chemistry B.

Supporting Table

Table S1. Primers Used in qRT-PCR.

Gene	**Forward primer**	**Reverse primer**
β-actin (human)	GGGAAATCGTGCGTGACATT	GGAACCGCTCATTGCCAAT
BAX (human)	TGGCAGCTGACATGTTTTCTG	TCCCGGAGGAAGTCCAATG
CASP3 (human)	AGAAATTGTGGAATTGATGCGTG	AGAAATTGTGGAATTGATGCGTG
SOD (human)	ATGGTGTGGCCGATGTGTCT	AAACGACTTCCAGCGTTTCCT
HMOX1 (human)	ACACCCAGGCAGAGAATGCT	CGAAGACTGGGCTCTCCTTGT
CAT (human)	GCTGAGGTTGAACAGATAGCCTTC	CACTCGAGCACGGTAGGGA
IL6 (human)	TGGCTGAAAAAGATGGATGCT	TCTGCACAGCTCTGGCTTGT

Table S2. P/TiO_2 NPs ICP-AES Characterization Results.

Chemical element	Element content
P	6.2940%
Ti	47.3884%

Table S3. Doping Amount of P in P/TiO_2 NPs.

Doping element	Actual doping amount	Theoretical doping amount
P	7.37%	16.67%

Supporting Figures

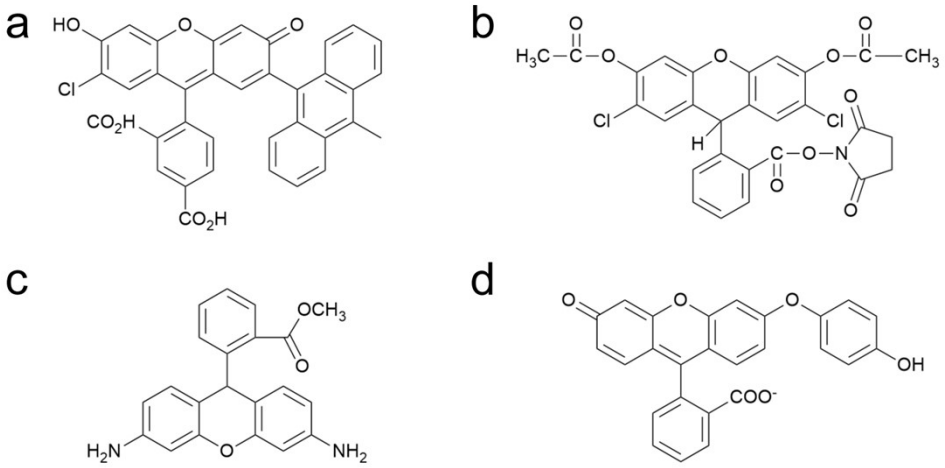

Figure S1. Chemical structure of fluorescence probes of $^1O_2$ (a), $\bullet O_2^-$ (b), H_2O_2 (c) and •OH (d).

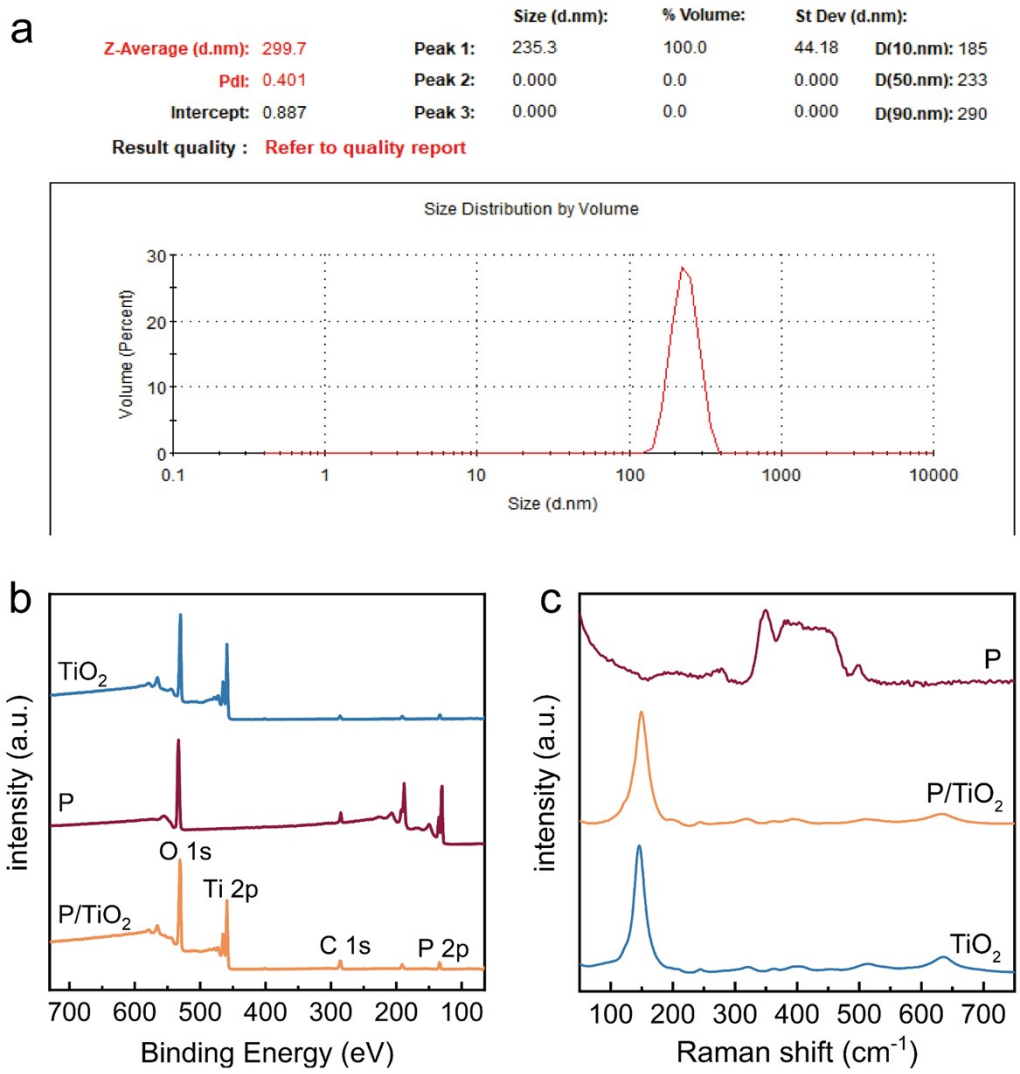

Figure S2. (a) Instrument-derived data for DLS size distribution of P/TiO_2 NPs. (b) XPS survey spectra of TiO_2, phosphorus and P/TiO_2 composites. (c) Raman spectra of TiO_2, phosphorus and P/TiO_2 composites.

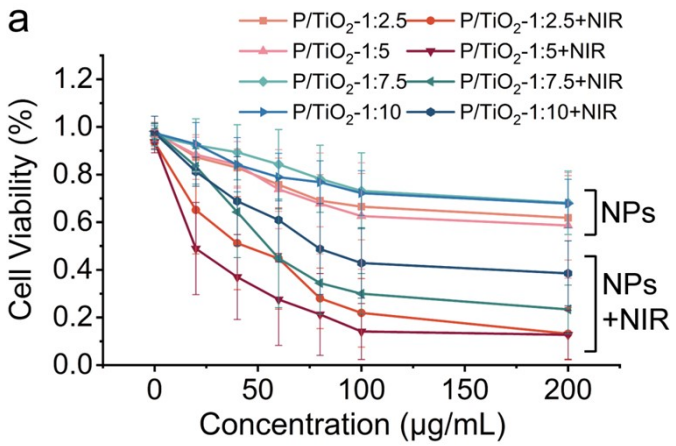

Figure S3. (a) The impact of different phosphorus doping ratios on the cytotoxicity of TiO_2 to 786-O cells in the presence or absence of NIR laser exposure. (P/TiO_2-1:x, x=2.5, 5, 7.5, 10)

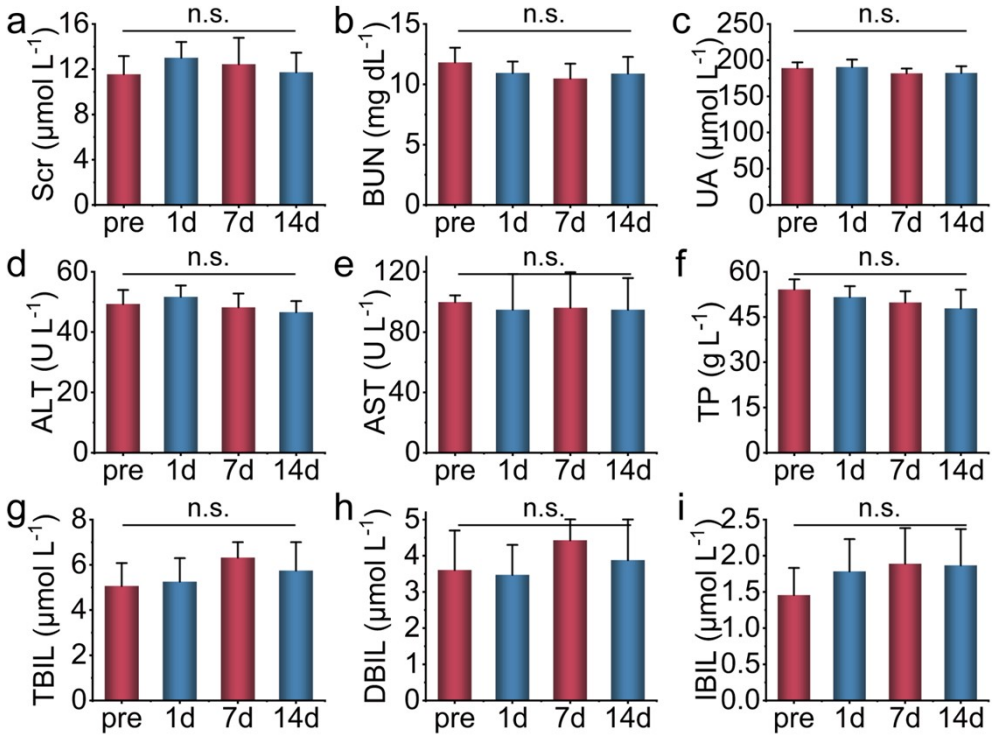

Figure S4. Blood biochemistry examinations (Scr (a), BUN (b), UA (c), ALT (d), AST (e), TP (f), TBIL (g), DBIL (h), IBIL (i)) of mice after intravenous injection with P/TiO_2 NPs for 1, 7, and 14 days. Scr, serum creatinine; BUN, blood urea nitrogen; UA, uric acid; ALT, glutamic pyruvic transaminase; AST, glutamic oxalacetic transaminase; TP, total protein; TBIL, total bilirubin; DBIL, direct bilirubin; IBIL, indirect bilirubin.

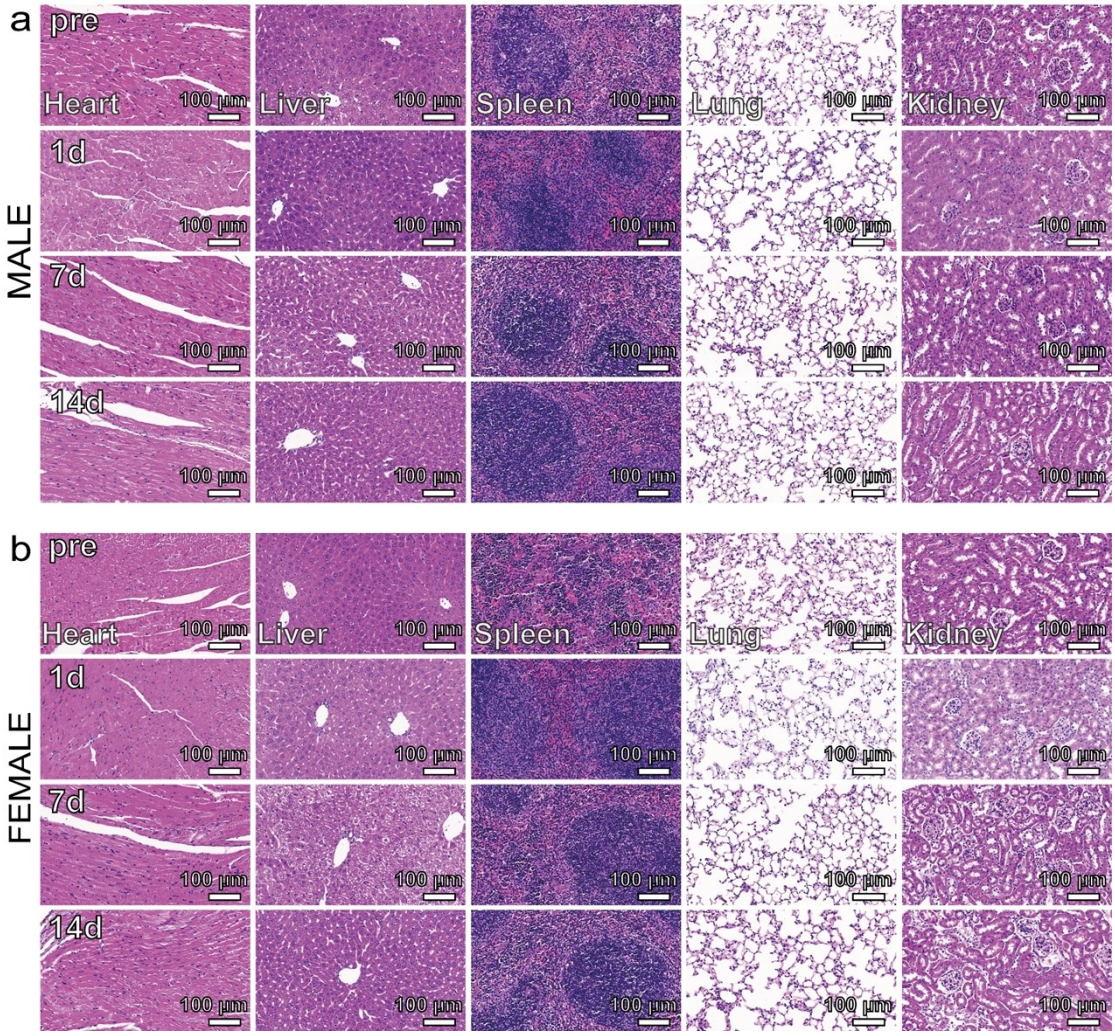

Figure S5. H&E staining studies of heart, liver, spleen, lung, and kidney tissues of male (a) and female (b) mice at 1, 7, and 14 d after intravenous injection of P/TiO_2 NPs.

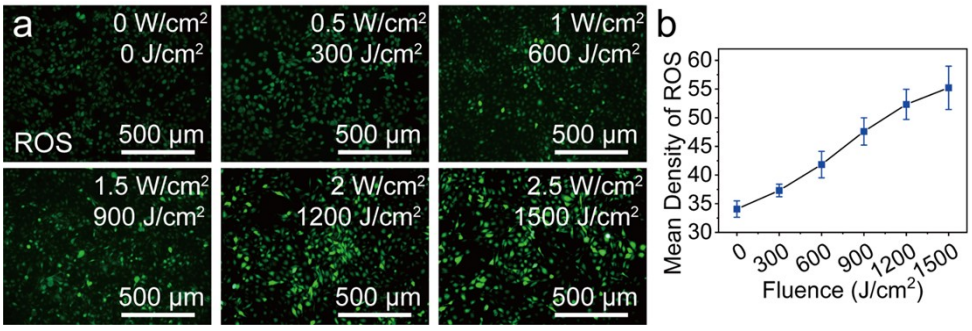

Figure S6. (a) Detection of ROS generation in 786-O cells by P/TiO_2 NPs after treatment with 808 nm NIR at different power densities/fluence for 10 min. (b) The fluorescence density was quantified by ImageJ software to establish the light dose response curve with increasing fluence.

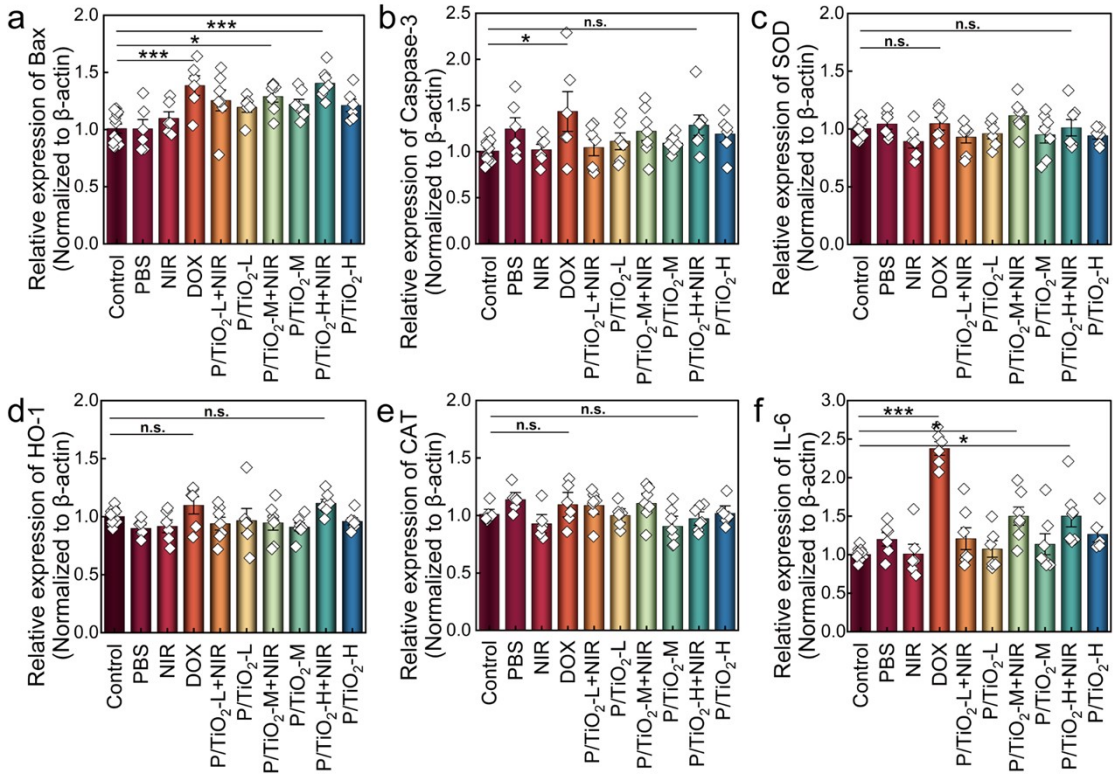

Figure S7. Changes of mRNA expression of Bax (a), Caspase-3 (b), SOD (c), HO-1 (d), CAT (e) and IL-6 (f) in HK-2 cells after P/TiO_2 NPs and PDT/PTT treatments. *: $p < 0.05$ and ***: $p < 0.001$ vs control.

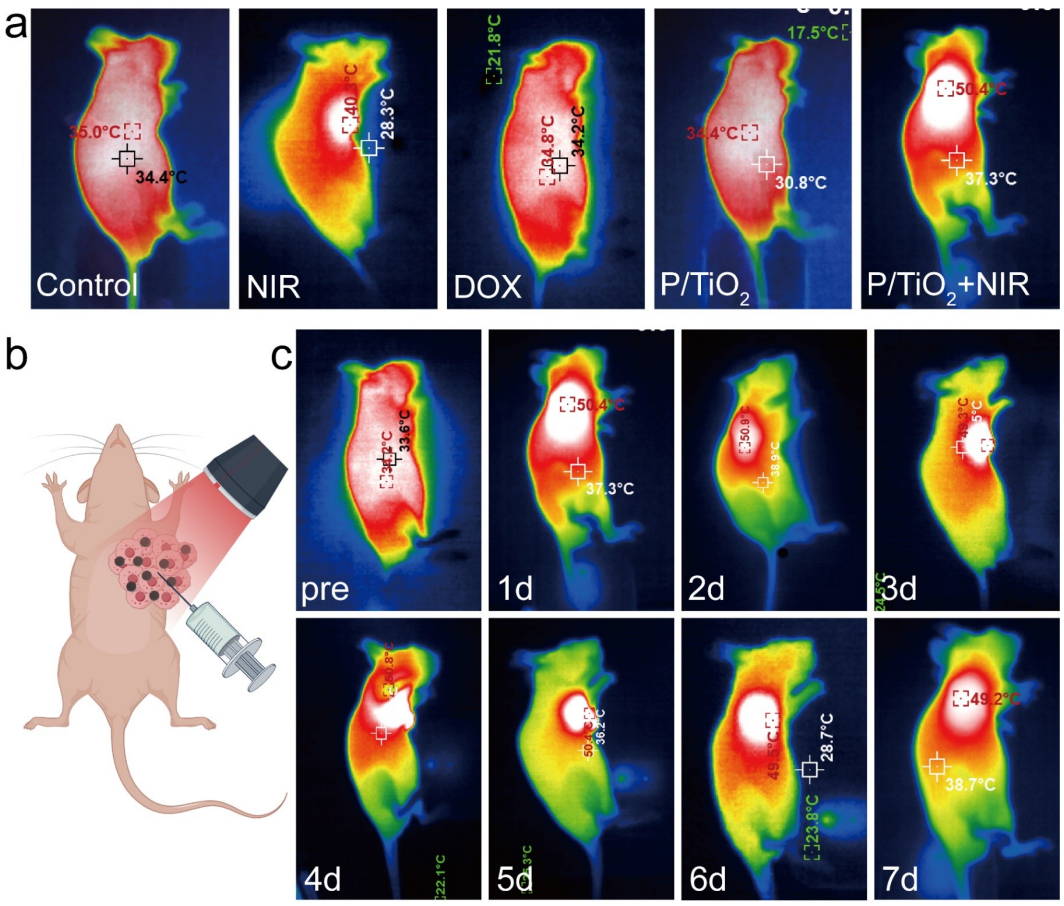

Figure S8. (a) and (c) Temperature images of different tumor-bearing mice. The maximum temperature was indicated respectively. (b) The pattern diagram of the animal research design.

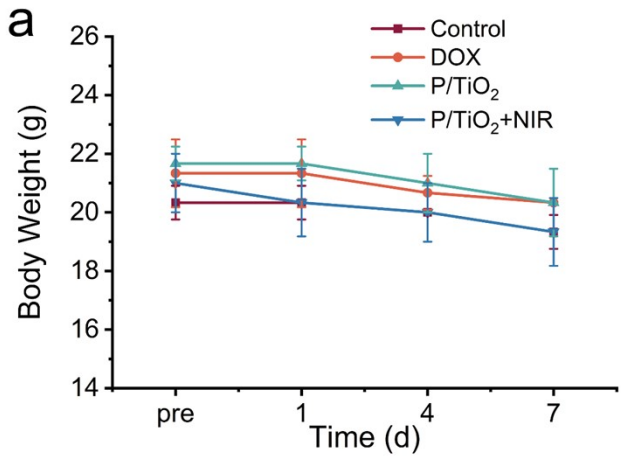

Figure S9. (a) Weight changes in tumor-bearing mice were treated with saline, DOX, P/TiO_2 NPs, and P/TiO_2 NPs+NIR for 7 days, respectively.

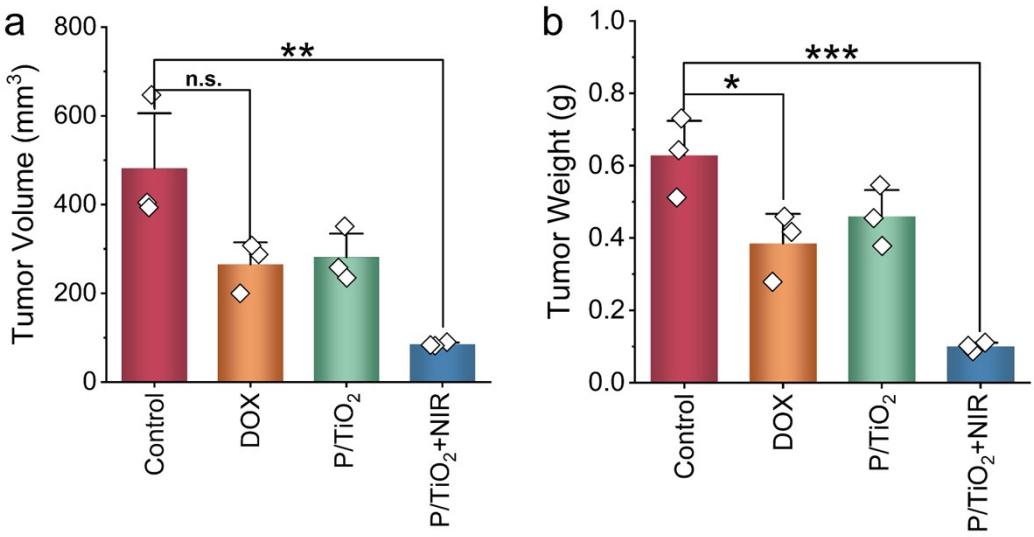

Figure S10. (a) Volumes and (b) weights of 786-O tumors after treatment with saline, DOX, P/TiO_2 NPs and P/TiO_2 NPs+NIR for 7 days, respectively.

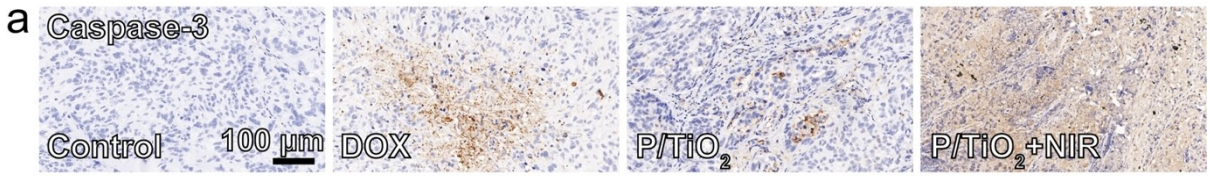

Figure S11. (a) Immunohistochemical evaluation of Caspase-3 in 786-O tumors post-treatment, where blue denotes nuclei and brown signifies Caspase-3 expression.